PHYSICAL REVIEW B VOLUME 15, NUMBER 4 15 FEBRUARY 1977

Effects of uniaxial stress on the electroreflectance spectrum of Ge and GaAs†

Meera Chandrasekhar*‡
Physics Department, Brown University, Providence, Rhode Island 02912

Fred H. Pollak
Physics Department, Belfer Graduate School of Science, Yeshiva University, New York, New York 10033
(Received 22 June 1976)

We have investigated the effects of static uniaxial compression along [001] and [111] on the Schottky-barrier electroreflectance spectrum of the $E_0 - E_0+\Delta_0$ and $E_1 - E_1+\Delta_1$ transitions in Ge and GaAs. From the stress-induced splittings and shifts of these optical structures we have obtained deformation potentials, spin-exchange parameters and reduced interband masses. For the $E_0 - E_0+\Delta_0$ transitions orbital (b_1 and d_1), spin-dependent (b_2 and d_2), and hydrostatic deformation potentials have been determined. In GaAs these are the first measurements reported for b_2 and d_2. The other parameters were found to be in good agreement with previous works. Interband reduced masses for the E_0 transition in Ge were determined at high stresses, in which case the degenerate valence band is split and the constant-energy surfaces are parabolic. Conclusive evidence for the existence of the electron-hole Coulomb interaction at 300°K as well as 77°K in the $E_1 - E_1+\Delta_1$ transitions has been obtained from the polarization-dependent stress-induced splittings for [001] stress. The observed splitting is not explained by one-electron theory but is accounted for by including the electron-hole exchange interaction. By including exciton effects at 300°K the systematic discrepancy between theory and experiment for the intensity and line shape of this structure should be resolved. In addition, deformation potentials due to shear (D_1^5), hydrostatic (D_1^1), and intraband (D_3^3) effects were determined for the $E_1 - E_1+\Delta_1$ transitions. The values obtained for D_1^5 in GaAs and Ge were found to be almost a factor of 2 larger than those previously reported. The reason for this is believed to be the higher resolution of the present experiments. Other parameters agree with prior works.

I. INTRODUCTION

Studies of the effects of uniaxial stress on the optical transitions of a material can yield valuable information about the intrinsic properties of the solid. The application of uniaxial stress and the related strain produce changes in the lattice parameter and the symmetry of the solid. These in turn, cause significant changes in the electronic band structure that manifest themselves in the optical properties. The anisotropic nature of the strain produces stress-induced splittings, and shifts of the energy levels, and oscillator strengths which can be related to the properties of the undeformed crystal.[1,2] From an analysis of these changes, including polarization and intensity effects, as a function of the magnitude and direction of the applied stress, we have been able to determine deformation potentials (both orbital and spin-dependent), symmetry characteristics, and information concerning the excitonic nature of the interband transitions.

The accurate study of interband transitions under stress have become possible with the advent of modulation spectroscopy,[3,4] in particular electroreflectance (ER).[5,6] The improved resolution of the Schottky-barrier electroreflectance (SBER) technique[7-9] and the consequent sharp, richly structured spectra has made possible a precise measurement of the effects of uniaxial stress on the electronic transitions in semiconductors.

In this study, two sets of transitions at different points in the Brillouin zone (BZ) in Ge and GaAs were investigated: the lowest direct transition at $\vec{k}=0$ (designated E_0) and its spin-orbit-split component ($E_0+\Delta_0$), and the next-higher direct transitions that occur in the $\Lambda(\langle 111\rangle)$ direction of the BZ(E_1) and its spin-orbit-split component ($E_1+\Delta_1$).[3,10] The transitions were studied at 77°K under uniaxial stress parallel to the [001] and [111] crystal directions using SBER. In addition, the $E_1 - E_1+\Delta_1$ structure was also studied at 300°K for stress $\vec{X}\parallel[001]$ in order to gain information concerning the excitonic nature of this transition at room temperature.[11]

Conclusive evidence for the existence of excitons in the $E_1 - E_1+\Delta_1$ transitions, both at room temperature and 77°K, has been obtained from these experiments for both Ge and GaAs. A polarization-dependent splitting is observed that cannot be explained on the basis of one-electron-band theory or by effects of reduced symmetry such as linear $\vec{k}$ terms in zinc-blende materials. The splitting can be accounted for only by including the spin exchange of excitons. The existence of contributions from the electron-hole Coulomb interaction to the $E_1 - E_1+\Delta_1$ transitions in diamond and zinc-blende-type (DZB) semiconductors has been suggested by several authors[12-17]. Theoretical calculations of $\epsilon_2(\omega)$ at room temperature, which do not include

excitonic contributions to the $E_1 - E_1 + \Delta_1$ transitions, show a systematic discrepancy both in intensity and line shape. The existence of excitons in the $E_1 - E_1 + \Delta_1$ transitions in GaAs at 77 °K was shown several years ago through a uniaxial-stress experiment.[18] The existence of the electron-hole interaction at 300 °K is shown in the present experiment. The evidence of this interaction is based solely on symmetry arguments and is not dependent on line-shape analysis. It is believed that this experiment resolves the controversy regarding the existence of electron-hole interaction in the $E_1 - E_1 + \Delta_1$ transitions at room temperature, and should also resolve the systematic discrepancy between theory and experiment in $\epsilon_2(\omega)$ in the region of this transition.[19-27]

In addition, the uniaxial stress experiments on the $E_1 - E_1 + \Delta_1$ transitions in Ge and GaAs have allowed us to make precise measurements of deformation potentials associated with both inter- and intraband effects. While the deformation potentials due to hydrostatic shifts and intraband mixing are found to be in reasonable agreement with other works, the interband-shear-deformation potential was measured to be almost a factor of 2 larger than values reported previously. The reason for this discrepancy is believed to be the increased resolution of the SBER technique, which permits clearly resolved splittings not well observed by earlier techniques.[28]

For the $E_0 - E_0 + \Delta_0$ transitions, in addition to orbital deformation potentials, it has been possible to measure the small spin-dependent shear-deformation potentials. These small quantities have been measured for the first time in GaAs, while the values for Ge are in good agreement with a previous determination.[29,30]

In addition to deformation potentials we have determined interband reduced masses from the Franz-Keldysh oscillations.[31] This measurement made for the E_0 structure is under high uniaxial stress, when the bands are no longer degenerate but are split by the reduced symmetry.

II. EXPERIMENTAL DETAILS

Standard techniques were used to measure SBER.[9,32] The incoming light beam was obtained by passing the output of a 200-W tungsten-halogen lamp through a $\frac{1}{4}$-m Jarell-Ash monochromator blazed at an appropriate wavelength. Light reflected from the face of the sample was collected into a photomultiplier with S-20 response for all experiments other than the $E_0 - E_0 + \Delta_0$ transitions in Ge, for which a PbS photoconducting cell was used. When a photomultiplier was used, a mechanical servo was used to keep the dc level of the output of the photomultiplier constant, so that measured signals directly gave $\Delta R/R$ (Ref. 2). A lock-in amplifier (Keithley 840 Autoloc) and a strip-chart recorder (Hewlett Packard 7101B) were used to analyze and record data.

Samples for SBER were prepared using conventional procedures from n-type single crystals of GaAs (6×10^{16} cm^{-3}) and Ge (4×10^{16} cm^{-3}).[32] Dimensions were typically $2\times2\times20$ mm^3. [110] faces were used for electroreflectance for both $\vec{X} \parallel [001]$ and $\vec{X} \parallel [111]$. A nickel film of about 40-Å thickness was evaporated onto the samples in order to form the Schottky barrier.

The stress rig used has been described previously.[1] Stresses reaching 10^{10} dyn cm^{-2} could be applied on both materials at 77 °K.

III. COMPARISON OF THEORY AND EXPERIMENTAL RESULTS

A. Lowest direction transitions at $\vec{k} = 0$: the $E_0 - E_0 + \Delta_0$ peaks

The lowest direct transitions in Ge and GaAs occur at the center of the BZ. In zinc-blende-type materials the presence of a term linear in $\vec{k}$ shifts band extrema slightly off $\vec{k} = 0$, but the term is small in magnitude[33] and its effects are not observed in the present experiments. In the absence of strain, the spin-orbit interaction splits the sixfold degenerate p-like valence-band multiplet into a fourfold $P_{3/2}$ multiplet ($J=\frac{3}{2}$, $M_J = \pm\frac{3}{2}, \pm\frac{1}{2}$) and a $P_{1/2}$ doublet ($J=\frac{1}{2}$, $M_J=\pm\frac{1}{2}$). The bands are labeled $v1(J=\frac{3}{2}, M_J=\pm\frac{1}{2})$, $v2(J=\frac{3}{2}, M_J=\pm\frac{3}{2})$, and $v3(J=\frac{1}{2}, M_J=\pm\frac{1}{2})$, as shown in Fig. 1. Transitions from the $P_{3/2}$ multiplet ($v1$ and $v2$ bands) to the s-like conduction band are labeled E_0, and from the $P_{1/2}$ doublet ($v3$ band), $E_0 + \Delta_0$. In GaAs, the E_0 and $E_0 + \Delta_0$

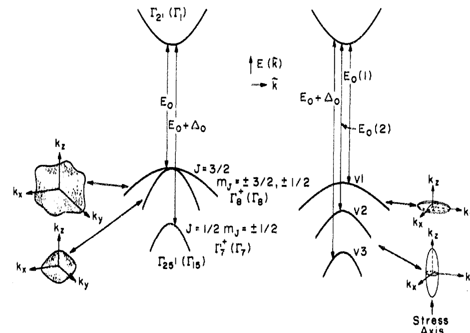

FIG. 1. Valence bands ($J=\frac{3}{2}$, $M_J=\pm\frac{3}{2}$, $\pm\frac{1}{2}$, and $J=\frac{1}{2}$, $M_J=\pm\frac{1}{2}$ in spherical notation) and lowest conduction band [$\Gamma_{2'}(\Gamma_1)$] in diamond- and zinc-blende-type semiconductors for unstrained (left-hand) and strained (right-hand) crystals. Also indicated is the double group for the spin-orbit-split bands in the unstressed case and the effects of strain on the warped energy surfaces.

transitions at 77 °K occur at 1.49 and 1.83 eV, respectively, and in Ge at 0.88 and 1.18 eV, respectively. Generally, the intensity of the $E_0+\Delta_0$ transition is about an order of magnitude lower than that of the E_0 peak.

The application of a uniaxial stress splits the degeneracy of the $v1$ and $v2$ bands, due to the reduced symmetry, and also produces a stress-induced coupling between the sets of $M_J=\pm\frac{1}{2}$ band ($v1$ and $v3$), causing a nonlinear stress dependence of these transitions. In addition, the hydrostatic pressure component of the strain results in an increase in energy of all transitions.

It has been shown that the total Hamiltonian for a p-like multiplet can be written as[1]

$$\mathcal{H}^{(i)}=\mathcal{H}_{so}^{(i)}+\mathcal{H}_1^{(i)}+\mathcal{H}_2^{(i)}, \tag{1}$$

where the superscript i is the band index, $\mathcal{H}_{so}$ is the spin-orbit Hamiltonian in the absence of strain, $\mathcal{H}_1$ is the orbital-strain Hamiltonian, and $\mathcal{H}_2$ is the stress-dependent spin-orbit Hamiltonian. In the following discussion the band index i will be suppressed.

Taking the valence-band wave function in the (J, M_J) representation the Hamiltonian matrix of Eq. (1) becomes

$$\begin{array}{ccc} v2 & v1 & v3 \\ |\frac{3}{2},\frac{3}{2}\rangle & |\frac{3}{2},\frac{1}{2}\rangle & |\frac{1}{2},\frac{1}{2}\rangle \end{array}$$

$$\begin{bmatrix} -\delta E_H-\frac{1}{2}\delta E_S & 0 & 0 \\ 0 & -\delta E_H+\frac{1}{2}\delta E_S & (1/\sqrt{2})\delta E_{S'} \\ 0 & (1/\sqrt{2})\delta E_{S'} & -\Delta_0-\delta E_{H'} \end{bmatrix}, \tag{2}$$

where Δ_0 is the spin-orbit splitting.

For $\vec{X}\parallel[001]$, the various terms in Eq. (2) are written as

$$\delta E_H^v=(a_1+a_2)(S_{11}+2S_{12})X=a(S_{11}+2S_{12})X, \tag{3a}$$

$$\delta E_{H'}^v=(a_1-2a_2)(S_{11}+2S_{12})X=a'(S_{11}+2S_{12})X, \tag{3b}$$

$$\delta E_S^{001}=2(b_1+2b_2)(S_{11}-S_{12})X=2b(S_{11}-S_{12})X, \tag{3c}$$

$$\delta E_{S'}^{001}=2(b_1-b_2)(S_{11}-S_{12})X=2b'(S_{11}-S_{12})X. \tag{3d}$$

For $\vec{X}\parallel[111]$, the hydrostatic pressure terms δE_H^v and $\delta E_{H'}^v$ remain the same while the shear terms δE_S and $\delta E_{S'}$ become

$$\delta E_S^{111}=(1/\sqrt{3})(d_1+2d_2)S_{44}X=(1/\sqrt{3})dS_{44}X, \tag{4a}$$

$$\delta E_{S'}^{111}=(1/\sqrt{3})(d_1-d_2)S_{44}X=(1/\sqrt{3})d'S_{44}X. \tag{4b}$$

In Eqs. (3) and (4), the quantities δE_H^v and $\delta E_{H'}^v$ represent shifts of the valence band due to the hydrostatic-pressure component of the strain, while δE_S^i and $\delta E_{S'}^i$ represent shear-induced splittings. The orbital (spin-dependent) deformation potentials are denoted by a_1 (a_2) for hydrostatic effects, and by b_1 (b_2) and d_1 (d_2) for shear effects due to tetragonal and rhombahedral symmetries, respectively, and the parameters S_{ij} are elastic compliance constants.

The Coulomb interaction and the consequent stress induced-mixing of the electron and hole wave functions is neglected for the $E_0-E_0+\Delta_0$ transitions. The effects of such a mixing term would cause a polarization dependent splitting, and has been seen in high-resolution experiments on the E_0 exciton.[1,34] The magnitude of this splitting (about 0.25 meV for GaAs) is below the resolution of our experiments. The term is included in the formulation for the $E_1-E_1+\Delta_1$ transitions where the splitting is considerably larger and cannot be neglected.

In the event that the stress-induced splittings and shifts are much smaller than the spin-orbit splitting Δ_0, the eigenvalues of Eq. (2) can be expanded in powers of X. This situation pertains in this experiment so that Eq. (2) can be written as

$$\delta E_{v2}=-\delta E_H^v-\tfrac{1}{2}\delta E_S, \tag{5a}$$

$$\delta E_{v1}=-\delta E_H^v+\tfrac{1}{2}\delta E_S+\tfrac{1}{2}(\delta E_{S'})^2/\Delta_0+\cdots, \tag{5b}$$

$$\delta E_{v3}=-\Delta_0-\delta E_{H'}^v-\tfrac{1}{2}(\delta E_{S'})^2/\Delta_0+\cdots, \tag{5c}$$

where δE_{vi} denotes the change in energy for the vi valence band due to the stress. The s-like conduction band does not split under the action of the stress, but does shift due to the hydrostatic-pressure component of the strain, an effect described by the deformation potential C_1.[35] Therefore, the stress dependence of the lowest direct gap, to first order in $\delta E_{S'}/\Delta_0$ is given by

$$\delta(E_c-E_{v2})=\delta E_H+\tfrac{1}{2}\delta E_S, \tag{6a}$$

$$\delta(E_c-E_{v1})=\delta E_H-\tfrac{1}{2}\delta E_S-\tfrac{1}{2}(\delta E_{S'})^2/\Delta_0+\cdots, \tag{6b}$$

$$\delta(E_c-E_{v3})=\Delta_0+\delta E_{H'}+\tfrac{1}{2}(\delta E_{S'})^2/\Delta_0+\cdots, \tag{6c}$$

where $\delta E_H=(C_1+a)(S_{11}+2S_{12})X$ and $\delta E_{H'}=(C_1+a')(S_{11}+2S_{12})X$.

Selection rules for the $E_0-E_0+\Delta_0$ transition have been calculated from the wave functions in Appendix A of Ref. 28. For light polarized parallel to the stress axis ($\vec{E}\parallel\vec{X}$), transitions from the $v1$ and $v3$ bands to the s-like conduction band are allowed. For light polarized perpendicular to the stress axis ($\vec{E}\perp\vec{X}$), transitions from all three bands are allowed.

The line shape of the E_0 structure both in GaAs and Ge is complicated by the superimposition of the sharp transverse exciton-polariton peak on the relatively broad interband transition. The amplitude, phase, and broadening of the spectral line shape associated with the exciton are extremely sensitive to the magnitude of the modulating voltage and the dc bias. The sensitivity is described by an interference effect.[8,36] At low modulation voltages, the

exciton spectrum is sharp and prominent, superimposed on the broader E_0 structure. As the modulation voltage is increased, the intensity of the interband transition increases and the amplitude of the exciton relative to the E_0 peak decreases, while the broadening of both the exciton and the interband transitions increase as the field goes beyond low-field limits. Due to the extreme sensitivity of the amplitude and phase of the exciton spectrum, it is possible to change the line shape of the exciton to be a prominent peak or to mask it within the interband structure by suitably adjusting the modulation voltage and dc bias. In GaAs, a low modulation voltage (typically 0.1 V rms) and a high negative bias (approximately −2.0 V), which maintains the surface in depletion, enhances the exciton so that it is about an order of magnitude larger than the E_0 structure. The other case of producing a smooth resultant curve from the E_0 and the exciton was usually achieved by low modulation voltage (0.1 V rms) and zero bias. Typical line shapes for the above cases are shown in the $X=0$ spectra (solid lines) in Figs. 2 and 3.

In GaAs, the broadening parameter was sufficiently large so that it is possible to work in the low-field regime, which is necessary to enhance the exciton over the interband transition. Henceforth, we shall refer to the exciton associated with the E_0 gap as Exciton. The Exciton and the combination of the Exciton and the E_0 interband transition (denoted by E_0 + Exciton) were studied separately under stress. For the $E_0+\Delta_0$ transition, the

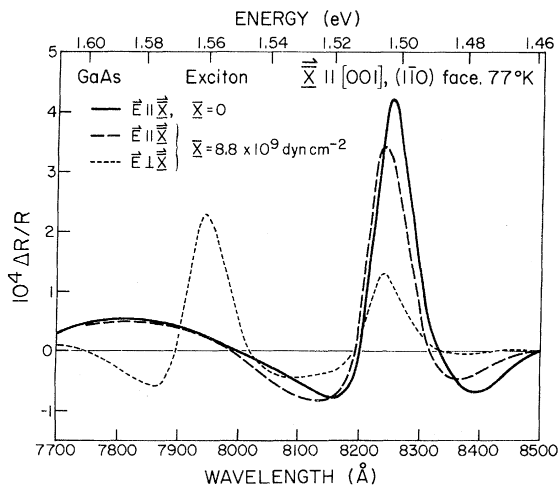

FIG. 2. Electroreflectance spectrum for the Exciton associated with the E_0 direct-band gap in GaAs at zero stress and $X=8.8\times10^9$ dyn cm^{-2} along [001] at 77 °K with light polarized parallel and perpendicular to the stress axis. The sample has been biased so that the Exciton is an order of magnitude larger than the interband transition.

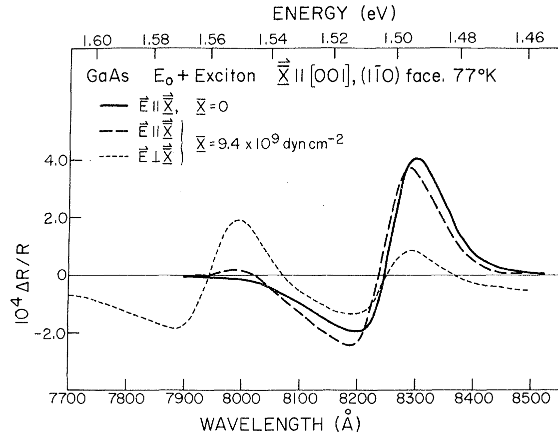

FIG. 3. Electroreflectance spectrum for the Exciton and interband transition of the E_0 direct gap in GaAs at zero stress and $X=9.4\times10^9$ dyn cm^{-2} along [001] at 77 °K with light polarized parallel and perpendicular to the stress axis. The sample has been biased so that the spectrum due to the Exciton and interband transition coincide into a smooth curve.

exciton associated with the structure was not seen at 77 °K. Indications of a weak excitonic structure for the $E_0+\Delta_0$ exist at 4 °K, and it is expected that this structure would be broadened beyond the limit of detectability at 77 °K. The interband $E_0+\Delta_0$ transition was investigated under stress. In general, the E_0 and the $E_0+\Delta_0$ were investigated on separate runs. Typically a modulation voltage of 0.1 V rms was used for the E_0 and 1.5 V rms for the $E_0+\Delta_0$, thus examining each transition in its low-field regime. The influence of piezoelectric strain in GaAs is assumed to be small. In order to verify this assumption, spectra were taken over a range of approximately one decade in the modulating voltage, and it was found that neither the spectral position nor the line shape changed. This defines the low-field regime and also shows that the piezoelectric effect is small.

In Ge, the lower transition energy and the smaller broadening parameter make it difficult to achieve low-field conditions. The sample was therefore biased so that the Exciton and the E_0 peaks coincided into a smooth curve. The modulation used was typically 0.8 V rms, − 1.0-V dc bias, taking the sample into the intermediate-field regime, where several Franz-Keldysh oscillations could be observed for both E_0 and $E_0+\Delta_0$ peaks. Typical line shapes are shown in the $X=0$ spectra of Fig. 4. The presence of a strong excitonic structure as well as the large number of Franz-Keldysh oscillations in Ge (up to 11 half-oscillations were observed for the E_0 structure) indicate that the electric field applied was uniform over the sample. The scattering, due to impurities and de-

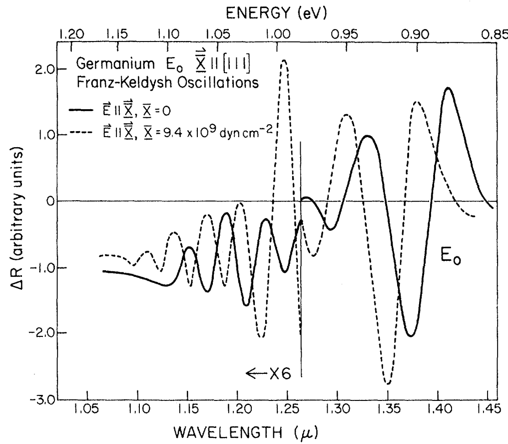

FIG. 4. Typical line shape of the E_0 electroreflectance structure of Ge at 77 °K for zero stress and a [111] stress of 9.4×10^9 dyn cm^{-2} showing the Franz-Keldysh oscillations. For zero stress (solid lines), an interference effect between bands of different masses is seen at the third and fourth half oscillations from the main E_0 structure. The height of the oscillations are substantially lower than the expected exponential-like decrease. At $X = 9.4 \times 10^9$ dyn cm^{-2}, the degenerate valence bands are separated, and a monotonic decrease in amplitude is observed.

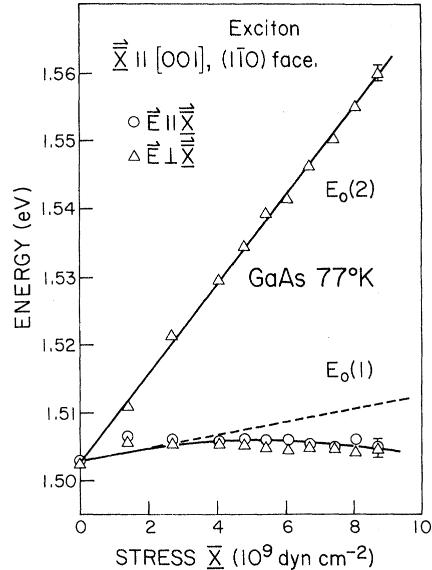

FIG. 5. Stress dependence of the energies of the direct-gap Exciton in GaAs at 77 °K for $\vec{X}$ || [001] with light polarized parallel and perpendicular to the stress axis. The dashed lines represent the linearized portion of the $E_0(1)$ stress dependence.

fects, is also expected to be very small for the above reason.

Shown in Figs. 2 and 3 are the electroreflectance spectra for GaAs of the Exciton and the E_0 + Exciton, respectively, for zero stress and stress along [001] with the electric-field vector of the incident light polarized parallel and perpendicular to the stress axis. The E_0 structure (either Exciton or E_0 + Exciton) is split by the action of the stress: for perpendicular polarization two transitions are seen, $E_0(1)$ and $E_0(2)$, while for parallel polarization only one peak, $E_0(1)$, is observed. The polarization selection rules indicate that $E_0(1)$ is caused by transitions from $v1$ to the conduction band, while $E_0(2)$ results from transition originating at $v2$ (see Fig. 1). Similar results have been observed for this stress direction in Ge and for $\vec{X}$ || [111] in GaAs and Ge.

In Figs. 5 and 6, we have plotted the energies of the Exciton and the E_0 + Exciton, as well as $E_0 + \Delta_0$, respectively, as a function of $\vec{X}$ || [001] for GaAs. The stress dependence of the $E_0 - E_0 + \Delta_0$ electroreflectance structure for $\vec{X}$ || [001] for Ge is shown in Fig. 7. The results of $\vec{X}$ || [111] for the Exciton, E_0 + Exciton, and $E_0 + \Delta_0$ for GaAs are displayed in Figs. 8 and 9 respectively. Figure 10 shows the stress dependence of the $E_0 - E_0 + \Delta_0$ structure for Ge for $\vec{X}$ || [111]. As discussed previously the E_0 structure for Ge was a combination of the exciton and interband transition, the modulation conditions being adjusted to give a smooth curve.

The above results show that the energy of $E_0(2)$ varies linearly with X while $E_0(1)$ and $E_0 + \Delta_0$ exhibit a nonlinear behavior at high stresses [see

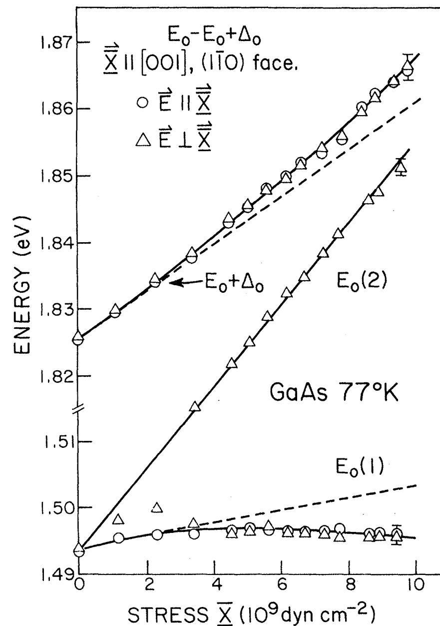

FIG. 6. Energies of the $E_0(1)$, $E_0(2)$, and $E_0 + \Delta_0$ peaks of the direct-gap interband electroreflectance structure of GaAs at 77 °K for $\vec{X}$ || [001] with light polarized parallel and perpendicular to the stress axis. The dashed lines represent the linearized portion of the curves.

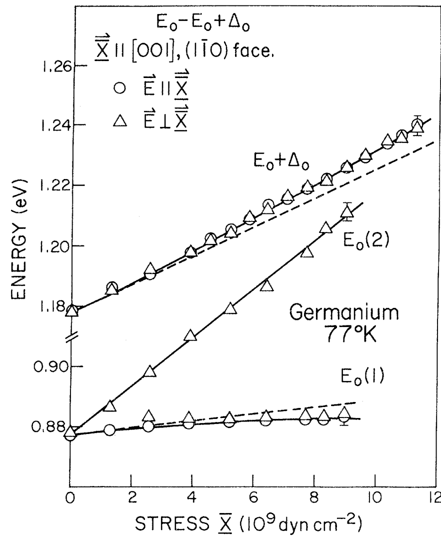

FIG. 7. Energies of the $E_0(1)$, $E_0(2)$, and $E_0+\Delta_0$ peaks of the direct-gap interband electroreflectance structure of Ge at 77 °K for $\vec{X}$ || [001] with light polarized parallel and perpendicular to the stress axis. The dashed lines represent the linearized portion of the $E_0(1)$ and $E_0+\Delta_0$ stress dependence.

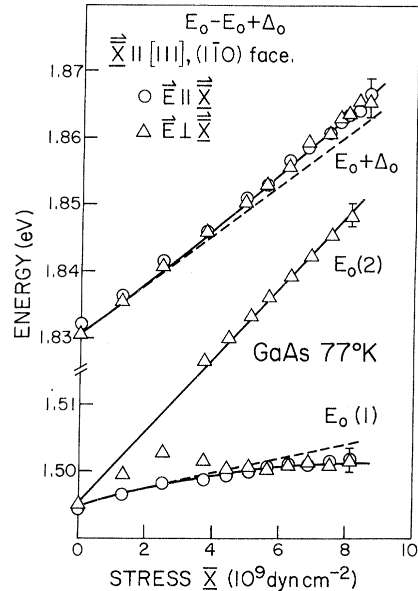

FIG. 9. Energies of the $E_0(1)$, $E_0(2)$, and $E_0+\Delta_0$ peaks of the direct-gap-interband electroreflectance structure of GaAs at 77 °K for $\vec{X}$ || [111] with light polarized parallel and perpendicular to the stress axis. The dashed line represent the linearized portion of the curves.

Eqs. (6)]. In order to evaluate the various deformation potentials the data was analyzed in the following manner. For the E_0 transition, the nonlinearity is determined first, giving for the two stress directions the deformation potentials $b'(=b_1 - b_2)$ and $d'(=d_1 - d_2)$ as indicated by Eqs. (3), (4), and (6). This nonlinear term is then subtracted from the $E_0(1)$ stress dependence resulting in the dashed lines in Figs. 5–10. The hydrostatic-deformation potential $C_1+a_1+a_2$ and the shear-deformation potentials $b(=b_1+2b_2)$ and $d(=d_1+2d_2)$ are

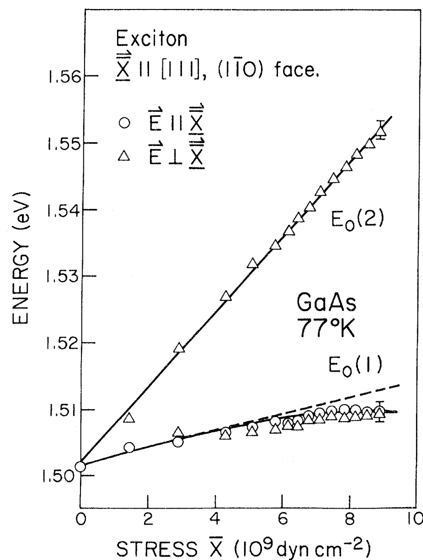

FIG. 8. Stress dependence of the energies of the direct-gap Exciton in GaAs at 77 °K for $\vec{X}$ [111] with light polarized parallel and perpendicular to the stress axis. The dashed lines represent the linearized portion of the $E_0(1)$ stress dependence.

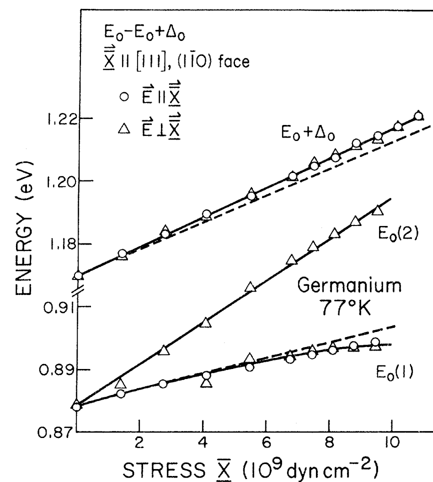

FIG. 10. Energies of the $E_0(1)$, $E_0(2)$, and $E_0+\Delta_0$ peaks of the direct-gap-interband electroreflectance structure of Ge at 77 °K for $\vec{X}$ || [111] with light polarized parallel and perpendicular to the stress axis. The dashed lines represent the linearized portion of the $E_0(1)$ and $E_0+\Delta_0$ stress dependence.

subsequently calculated from the shift of the center of gravity and splitting, respectively, of the linearized stress dependence. For the $E_0+\Delta_0$ structure the nonlinearity gives b' and d' (for $\vec{X}\parallel[001]$ and $\vec{X}\parallel[111]$, respectively) while the linear shift (dashed lines in Figs. 6, 7, 9, and 10) gives the hydrostatic parameter $C_1+a_1-2a_2$. The values of b' and d' obtained from the stress-dependence of $E_0+\Delta_0$ are in good agreement with those obtained from the E_0 transition. In all cases, the tabulated values of the deformation potentials were calculated using a least-squares fit. No attempt was made to determine C_1+a_1 and a_2 uniquely due to the experimental uncertainties in the values obtained from the hydrostatic component. As will be discussed in more detail below the value of a_2 is expected to be small.

The deformation potentials obtained in GaAs for the Exciton alone, and for the sum of the E_0 interband transition and the Exciton, are in good agreement. Though the binding energy of the Exciton is expected to change with stress, this change is

TABLE I. Deformation potentials (in eV) for the $E_0-E_0+\Delta_0$ transitions in germanium.

	Present work	Previous work	Theoretical calculations
$C_1+a_1+a_2$	-10.9 ± 0.8 [a,b]	-9.4 ± 0.4 [c]	-12.8 [d]
	-10.3 ± 0.8 [e,b]	-10.0 ± 0.8 [f]	-10.6 [d]
		-10.5 ± 1.1 [g]	-8.8 [h]
		-8.1 [i], 11.0 ± 0.7 [j]	-10.3 [k]
		-10.1 ± 0.2 [l]	
$C_1+a_1-2a_2$	-11.2 ± 1.0 [a,m]		
	-10.3 ± 1.0 [e,m]		
$b=b_1+2b_2$	-2.86 ± 0.15 [a,b]	-2.6 ± 0.2 [c], -2.7 ± 0.3 [g]	-2.3 [d]
		-2.4 ± 0.2 [i], -1.8 ± 0.2 [n]	-2.3 [n]
		-2.1 ± 0.2 [o], $-2.21\pm.13$ [p]	
		-2.4 ± 0.1 [l],	
$b'=b_1-b_2$	-2.44 ± 0.15 [a,b]	$-1.54\pm.11$ [p]	
	-2.44 ± 0.20 [a,m]		
b_1	-2.58 ± 0.12 [a,b]	-1.77 ± 0.12 [p]	
b_2	-0.14 ± 0.08 [a,b]	-0.22 ± 0.04 [p]	
$d=d_1+2d_2$	-5.28 ± 0.50 [e,b]	-4.7 ± 0.3 [c], -4.7 ± 0.5 [g]	-5.6 [d]
		-4.1 ± 0.4 [i], -7.0 ± 1.5 [o]	-4.9 [h]
		-6.0 ± 0.6 [q], -4.4 ± 0.27 [p]	
$d'=d_1-d_2$	-3.98 ± 0.4 [e,b]	-3.24 ± 0.23 [p]	
	-4.03 ± 0.6 [e,m]		
d_1	-4.41 ± 0.20 [e,b]	-3.63 ± 0.25 [p]	
d_2	-0.43 ± 0.15 [a,b]	-0.39 ± 0.09 [p]	

[a] $\vec{X}\parallel[001]$.
[b] E_0 peak.
[c] Reference 28.
[d] P. J. Melz, Technical Report HP-25, Harvard University, Division of Engineering and Applied Physics, Cambridge, Mass. (unpublished).
[e] $\vec{X}\parallel[111]$.
[f] J. Feinleib, S. Groves, W. Paul, and R. Zallen, Phys. Rev. 131, 2070 (1963); R. Zallen and W. Paul, Phys. Rev. 134, A1628 (1964).
[g] A. M. Glass, Can. J. Phys. 43, 12 (1965).
[h] L. R. Saravia and D. Brust, Phys. Rev. 178, 1240 (1969).
[i] I. Balslev, Solid State Commun. 5, 315 (1967).
[j] Reference 37.
[k] F. Herman, R. Kortum, C. D. Kuglin, and R. A. Short, in *Quantum Theory of Atoms, Molecules and Solids: A Tribute to J. C. Slater*, edited by Per-Olov Lowdin (Academic, New York, 1966), p. 381.
[l] G. Bordue, G. Alibert, and M. Averous, in *Proceedings of the Eleventh International Conference on The Physics of Semiconductors, Warsaw, 1972* (PWN-Polish Scientific, Warsaw, 1972), p. 1426.
[m] $E_0+\Delta_0$ peak.
[n] I. Balslev, Phys. Rev. 143, 636 (1966).
[o] J. J. Hall, Phys. Rev. 128, 68 (1962).
[p] Reference 30.
[q] J. C. Hensel, Solid State Commun. 4, 231 (1966).

negligible compared to the splittings and shifts due to the removal of degeneracy in the valence band. A comparison of the energy versus stress curves for the Exciton and the E_0 + Exciton (Figs. 5, 6, 8, and 9) indicated that the Exciton follows the band edge closely. This result shows that for Ge, in which case it was not possible to measure the Exciton and E_0 + Exciton separately, the spectral information is not distorted by the effects of stress on the Exciton.

Listed in Tables I and II are the various deformation potentials of the direct gap for Ge and GaAs, respectively. These values are compared with those obtained by other experimental techniques such as piezoreflectance, hydrostatic pressure, electrolyte electroreflectance, cyclotron resonance, etc., and are generally in good agreement with previous works. In addition, we have listed values of certain of those parameters obtained from theoretical calculations.

TABLE II. Deformation potentials (in eV) of the $E_0 - E_0 + \Delta_0$ transitions in gallium arsenide.

	Present work	Previous work	Theoretical calculations
$C_1 + a_1 + a_2$	-8.93 ± 0.9 [a,b]	-9.0 ± 0.4 [c]	-15.3 [d]
	-8.38 ± 0.8 [a,e]	-9.0 ± 0.9 [f]	-15.2 [d]
	-8.14 ± 0.8 [g,b]	-9.2 ± 0.5 [h]	
	-8.07 ± 0.8 [g,e]	-8.2 [i]	
		-9.0 [j]	
$C_1 + a_1 - 2a_2$	-8.27 ± 0.6 [a,k]		
	-7.80 ± 0.6 [j,k]		
$b = b_1 + 2b_2$	-1.76 ± 0.1 [a,b]	-2.0 ± 0.2 [c]	-0.4 [d]
	-1.66 ± 0.1 [a,e]	-1.96 ± 0.1 [h]	
		-1.7 ± 0.2 [i]	
$b' = b_1 - b_2$	-2.73 ± 0.2 [a,b]		
	-2.47 ± 0.2 [a,e]		
	-2.11 ± 0.36 [a,k]		
b_1	-2.41 ± 0.15 [a,b]		
	-2.29 ± 0.15 [a,e]		
b_2	$+0.32 \pm 0.1$ [a,b]		
	$+0.27 \pm 0.1$ [a,e]		
$d = d_1 + 2d_2$	-4.59 ± 0.25 [g,b]	-6.0 ± 0.4 [c]	-3.0 [d]
	-4.52 ± 0.25 [g,e]	-5.4 ± 0.3 [h]	
		-4.4 ± 0.6 [i]	
$d' = d_1 - d_2$	-5.34 ± 0.4 [g,b]		
	-5.74 ± 0.4 [g,e]		
	-6.4 ± 0.7 [g,k]		
d_1	-5.09 ± 0.2 [g,b]		
	-5.33 ± 0.2 [g,e]		
d_2	$+0.25 \pm 0.16$ [g,b]		
	$+0.41 \pm 0.16$ [g,e]		

[a] $\vec{X} \parallel [001]$.
[b] Exciton (E_0).
[c] Reference 28.
[d] P. J. Melz, Technical Report HP-25, Harvard University, Div. of Engineering and Applied Physics, Cambridge, Mass (unpublished).
[e] E_0 peak.
[f] J. Feinleib, S. Groves, W. Paul, and R. Zallen, Phys. Rev. 131, 2070 (1963); R. Zallen and W. Paul, Phys. Rev. 134 A1628 (1964).
[g] $\vec{X} \parallel [111]$.
[h] R. N. Bhargava and M. Nathan, Phys. Rev. 161, 695 (1967).
[i] I. Balslev, Solid State Commun. 5, 315 (1967).
[j] M. I. Wolfe, Thesis (Yeshiva University, 1973) (unpublished).
[k] $E_0 + \Delta_0$ peak.

The hydrostatic and shear-deformation potentials have been measured previously by several different techniques. The spin-dependent hydrostatic-deformation potential a_2 has been measured by hydrostatic-pressure techniques to be 0.03 ± 0.03 in Ge,[37] and -0.04 ± 0.06 in GaAs,[38] quantities difficult to determine in the present experiment. The spin-dependent shear-deformation potentials b_2 and d_2 are measured for the first time in GaAs. In Ge, these deformation potentials have been measured by Hensel and Suzuki using cyclotron resonance in p-type material.[30] The second-order nature of these parameters make them difficult to measure in interband transitions, but it was still possible to obtain values for them that are in reasonably good agreement with those obtained in cyclotron resonance. It should be noted that there is a difference in sign of these parameters in GaAs relative to Ge and Si,[39] an effect which is not understood at present.

A theoretical estimate for a_2, the change in spin-orbit splitting Δ_0 due to the hydrostatic component of the strain can be written as

$$(\delta\Delta_0/\Delta_0) = -\eta(\delta a_l/a_l), \tag{7}$$

where a_l is the lattice constant and η is a dimensionless constant, so that

$$a_2 = -\tfrac{1}{9}\eta\Delta_0. \tag{8}$$

Estimates for η have been made for Ge using different techniques yielding a range of values for η: Brust and Liu $\eta = 4$ (at L),[40] Cerderia *et al.* $\eta = 1.7$,[41] Melz and Ortenburger $\eta = 1.8$,[37] Wepfer *et al.* $\eta = 0.2$,[42] and Hensel and Suzuki $\eta = 2$.[29,30] Assuming a value of $\eta = 2$, we arrive at $a_2 = 0.06$ eV for Ge. Assuming the same coefficient for GaAs, $a_2 = 0.07$ eV. It is clear that the estimated value of a_2 is less than 1% of a_1, putting it below the accuracy of the present experiment.

The theory for b_2 and d_2 are not well understood at present. Using the deformable-ion model, not assuming any mixing between bands, Hensel and Suzuki[29,30] calculate a partial numerical estimate for Ge of $b_2 \sim \frac{1}{9}\Delta_0 = 0.03$ eV, $d_2 \sim -(1/3\sqrt{3})\Delta_0 = -0.05$ eV, values an order of magnitude lower than those obtained experimentally. It is known that mixing occurs between bands, giving a first-order matrix element containing the change in

crystal potential due to strain, and a second-order term containing matrix elements with the spin-orbit interaction and the strain interaction connecting the valence states with several conduction states.

Interband effective masses were obtained from an analysis of the period of the Franz-Keldysh oscillations seen for E_0 and $E_0+\Delta_0$ in Ge.[31] From classical Franz-Keldysh theory, the energy at the peak of the νth half oscillation is correlated to a phase change of π from the $(\nu-1)$th half oscillation, so that[43]

$$\nu\pi = \theta + \tfrac{2}{3}[(E_\nu - E_g)/\hbar\Omega]^{3/2}, \qquad (9)$$

where ν is the extremum number, E_ν is the energy of the peak, E_g is the transition energy, $\hbar\Omega$ is the characteristic energy of the transition given by

$$(\hbar\Omega)^3 = \frac{e^2\hbar^2\mathcal{E}^2}{8\mu_\parallel}, \qquad (10)$$

where $\mathcal{E}$ is the electric field and $\mu_\parallel$ is the reduced mass in the direction of $\vec{\mathcal{E}}$. A plot of extremum ν versus $(\hbar\omega - E_g)_\nu^{3/2}$ yields a slope proportional to $(\hbar\Omega)^{-3/2} \sim (\mu_\parallel/\mathcal{E}^2)^{1/2}$ (Figs. 11 and 12). The E_0 and $E_0+\Delta_0$ spectra have been taken under identical field conditions, so the field $\mathcal{E}$ may be determined from the $E_0+\Delta_0$ oscillations assuming $\mu_\parallel$. This permits a calculation $\mu_\parallel$ for E_0. Figure 4 shows the typical line shapes of Franz-Keldysh oscillations seen for the E_0 structure in Ge. The E_0 oscillations have a contribution from the light- and the heavy-hole bands. At zero stress the oscillations seen are the combination of the contribution from both bands, the amplitudes showing interference at a point where the amplitudes of the oscillations from the light- and heavy-hole bands cancel each other. This is seen in the $X=0$ plot in Fig. 4 (solid lines). At high stresses the bands are separated, and the reduced masses for the two bands may be separately found. The light-hole $M_J=\pm\frac{3}{2}$ band is seen for $\vec{E}\perp\vec{X}$, well separated from the heavy-hole $M_J=\pm\frac{1}{2}$ band so that there is little interference between them. Figure 4 also shows the oscillations for the $v1$ band at high stresses and the absence of interference is clear. $\mu_\parallel$ for the $M_J=\pm\frac{1}{2}$ may be determined from the $\vec{E}\parallel\vec{X}$ spectrum, where the $M_J=\pm\frac{3}{2}$ band is not seen (Figs. 11 and 12).

The slopes used to calculate the reduced masses are proportional to the square root of $\mu_\parallel$ and therefore tend to be relatively insensitive to changes in the reduced mass. Again, since the electric field tends to mix states of different $\vec{k}$, the masses obtained would be an average over a small spread of reduced masses about $\vec{k}=0$. The values of $\mu_\parallel$ obtained for high stresses in Ge are listed in Table III. The ratios of $\mu_{1/2}/\mu_{3/2}$ are also calculated in order to reduce the uncertainty caused by eliminating the $\mathcal{E}^2$ term using the oscillations of $E_0+\Delta_0$, which have larger errors due to the weaker nature of the transition and a smaller number of oscillations. The values obtained for the reduced masses are compared with work by Hensel and Suzuki[29,30] in cyclotron resonance of the valence bands, which occurs at $\vec{k}=0$. The conduction-band mass is assumed to remain unchanged under uniaxial stress. The effective-mass values assumed are $m_c^*=0.038$ for the conduction band and $m^*=0.077$ for the spin-

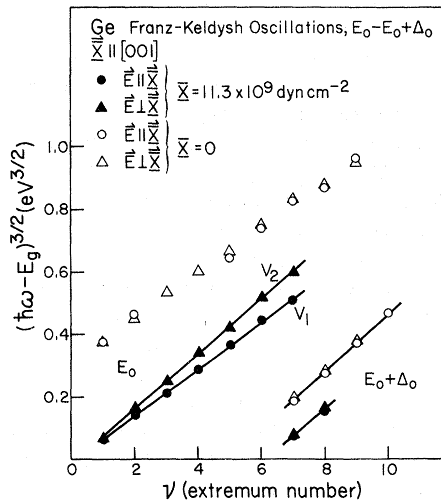

FIG. 11. Fits for the determination of the interband reduced masses from the Franz-Keldysh oscillations of the E_0 and $E_0+\Delta_0$ transitions in Ge at 77 °K for $X=0$ and 11.3×10^9 dyn cm^{-2} along [001].

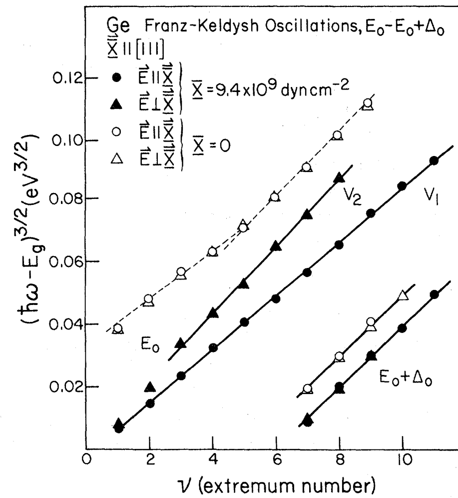

FIG. 12. Fits for the determination of the interband reduced masses from the Franz-Keldysh oscillation of the E_0 and $E_0+\Delta_0$ transitions in Ge at 77 °K for $X=0$ and 9.4×10^9 dyn cm^{-2} along [111]. The interference between the masses at zero stress for the E_0 structure can be seen as a break in the curve.

TABLE III. Reduced masses of the E_0 transition in germanium (in units of free electron mass).

	Present work	Previous work
$\mu_{1/2}$	0.037 ± 0.004 [a]	0.027 [a,b]
	0.033 ± 0.002 [c]	0.028 [c,b]
		0.028 [d,b], 0.029 [e,b]
		0.038 [f]
$\mu_{3/2}$	0.028 ± 0.003 [a]	0.022 [a,b], 0.022 [d,b]
	0.022 ± 0.002 [c]	0.022 [c,b], 0.022 [e,b]
		0.022 [f]
$\mu_{1/2}/\mu_{3/2}$	1.32 ± 0.13 [a]	1.25 [a,b]
	1.50 ± 0.15 [c]	1.30 [c,b]
		1.73 [f,d]

[a] $\vec{X} \parallel [001]$ at 11.3×10^9 dyn cm^{-2}.
[b] Reference 30.
[c] $\vec{X} \parallel [111]$ at 9.43×10^9 dyn cm^{-2}.
[d] $\vec{X} \parallel [001]$ at $\vec{X}=0$.
[e] $\vec{X} \parallel [111]$ at $\vec{X}=0$.
[f] Reference 31.

orbit-split valence band, in units of electron rest mass. $\mu_{\parallel}$ for the $E_0+\Delta_0$ band is therefore 0.025.

B. Transitions off $\vec{k}=0$: the Λ transitions $E_1 - E_1 + \Delta_1$

For band extrema or interband critical points at $\vec{k}\neq 0$, the shear component of the applied uniaxial stress can cause three effects: (i) band states of different $\vec{k}$ vector, which are degenerate because of crystal symmetry, may have their degeneracy reduced depending on the projections of their $\vec{k}$ vectors onto the stress direction (intraband splitting), (ii) a splitting of the degenerate orbital bands whose $\vec{k}$ vectors are not parallel to the stress, and (iii) a stress-induced coupling between neighboring bands [i.e., the Δ_1 conduction-band minima and nearby $\Delta_{2'}'$ band in silicon].[1] The second and third effects mentioned above are denoted as intraband splittings. In addition to these shear effects there is a shift due to the hydrostatic component of the strain.

In Ge and GaAs, the next significant structure in the optical spectrum above the direct edge is due to transitions which occur along the eight equivalent $\langle 111\rangle$ directions $(\Lambda_3-\Lambda_1)$ of the BZ. These transitions have been labeled $E_1 - E_1+\Delta_1$. Since uniaxial stress does not remove the inversion symmetry of the crystal only the four equivalent transitions along the [111], $[\bar{1}\bar{1}1]$, $[1\bar{1}\bar{1}]$, and $[\bar{1}1\bar{1}]$ directions need be considered. The application of a uniaxial stress along [001] does not remove the $\vec{k}$-space degeneracy of these bands (no interband splitting) but does cause an intraband effect, i.e., the stress-dependent splitting of the Λ_3 orbital bands. A [111] stress produces both an inter- and intraband splitting: the [111] band is split off from the remaining three bands ($[\bar{1}\bar{1}1]$, $[1\bar{1}\bar{1}]$, and $[\bar{1}1\bar{1}]$), and there is an intraband effect on this latter group whose $\vec{k}$ vector does not lie along the stress direction. In addition to these one-electron effects an electron-hole Coulomb interaction may be present which will be affected by the stress.

The strain Hamiltonian for $\langle 111\rangle$ transitions has been discussed in the literature.[1] We will use the deformation potentials in Kane's notation, i.e., D_1^1 (hydrostatic), D_1^5 (interband shear), D_3^3, and D_3^5 (intraband-deformation potentials appropriate to strains of tetragonal and rhombohedral symmetries, respectively).[44] Spin exchange due to the electron-hole interaction is included by means of the Elliot exchange term.[13,32,45] The effect of the spin-exchange interaction is quite pronounced for the case of $\vec{X}\parallel[001]$, causing polarization-dependent splittings. For $\vec{X}\parallel[111]$, however, no effects related to the spin-exchange term have been observed and therefore is not included in the formulation given below.

1. Stress parallel to [001]

It has been demonstrated that the combined strain and spin-exchange Hamiltonian for $\vec{X}\parallel[001]$, using the appropriate exciton wave functions as a basis, has the form[11,18]

$$\begin{array}{cccc} \Lambda_{3\bar{x}}^{E_1} & \Lambda_{3\bar{x}}^{E_1+\Delta_1} & \Lambda_{3\bar{y}}^{E_1} & \Lambda_{3\bar{y}}^{E_1+\Delta_1} \end{array}$$
$$\begin{bmatrix} E_1+\delta_H & \delta_J-\delta_S & 0 & 0 \\ \delta_J-\delta_S & E_1+\Delta_1+\delta_H & 0 & 0 \\ 0 & 0 & E_1+\delta_H & \delta_J+\delta_S \\ 0 & 0 & \delta_J+\delta_S & E_1+\Delta_1+\delta_H \end{bmatrix}, \quad (11)$$

where δ_H and δ_S are the matrix elements due to the hydrostatic and shear strain, respectively, while the quantity δ_J is the matrix element of the electron-hole exchange interaction. The quantity $\Lambda_{3\bar{x}}$ and $\Lambda_{3\bar{y}}$ represent appropriate linear combinations of exciton wave functions to yield states polarized in the $\bar{x}$ ([110]) and $\bar{y}$ ($[1\bar{1}0]$) directions. The strain dependence of the exchange interactions has been neglected. Since a [001] stress affects all $\langle 111\rangle$ transitions equally, the summation over equivalent bands is trivial provided the valley orbit splitting is neglected.

In Eq. (11) the exchange term can be written as

$$\delta_J = P(0)J, \quad (12)$$

where $P(0)$ is the probability that the electron and the hole are on the same lattice site and J is the exchange interaction between Wannier functions. The strain terms are

$$\delta_H = (D_1^1/\sqrt{3})(S_{11}+2S_{12})X, \quad (13)$$

and

$$\delta_S = (\tfrac{2}{3})^{1/2} D_3^3 (S_{11} - S_{12}) X, \qquad (14)$$

where D_1^1 and D_3^3 are the one-electron deformation potentials.

By solving Eq. (11) the exciton energies as a function of X can be written as

$$E(X) = E_1 + \tfrac{1}{2}\Delta_1 + \delta_H \pm [(\tfrac{1}{2}\Delta_1)^2 + (\delta_J \pm \delta_S)^2]^{1/2}. \qquad (15)$$

Under the conditions that $\Delta_1 \gg \delta_S \gg \delta_J$ (which holds for both Ge and GaAs), Eq. (4) can be expanded to yield

$$E_1(X) = E_1 + \delta_H - (\delta_S^2 \pm 2\delta_S \delta_{J1})/\Delta_1 + \cdots, \qquad (16a)$$

and

$$E_1 + \Delta_1(X) = E_1 + \Delta_1 + \delta_H + (\delta_S^2 \pm 2\delta_S \delta_{J2})/\Delta_1 . \qquad (16b)$$

In Eqs. (16a) and (16b) we have taken into account the experimentally observed fact that E_1 and $E_1 + \Delta_1$ have different spin-exchange interactions.

We have measured the effects of $\vec{X} \parallel [001]$ on the $E_1 - E_1 + \Delta_1$ electroreflectance structure of Ge and GaAs at both 77 and 300 °K. Shown in Figs. 13 and 14 are the spectra for Ge at 77 and 300 °K, respectively, while in Figs. 15 and 16 we have plotted the spectra for GaAs at 77 and 300 °K, respectively. The data has been plotted for both $\vec{E} \parallel \vec{X}$ and $\vec{E} \perp \vec{X}$. In all cases the applied modulation voltage was kept low enough not to cause a field-dependent broadening of the structure. Typically, these values were 25 and 3 V for Ge at 77 and 300 °K, respectively, and 4 and 2 V for GaAs at 77 and 300 °K, respectively. The above figures show that the applied stress causes a shift in gravity of the $E_1 - E_1 + \Delta_1$ peaks, an increase in the energy separation between these two peaks and a small polarization-dependent splitting for each optical structure. The polarization-dependent splitting is such that, for the E_1 transition, the component for $\vec{E} \parallel \vec{X}$ occurs at a higher energy than the $\vec{E} \perp \vec{X}$ component while for the $E_1 + \Delta_1$ structure the ordering is reversed. The selection rules are in agreement with Eqs. (11) and (16). This polarization-dependent splitting has been observed before in GaAs at 77 °K using wavelength modulation.[18] Since $\vec{X} \parallel [001]$ removes neither the degeneracy of the ⟨111⟩ valleys nor the Kramer's degeneracy, the one-electron theory is unable to explain the existence of this splitting. Also it is not possible to account for the effect in

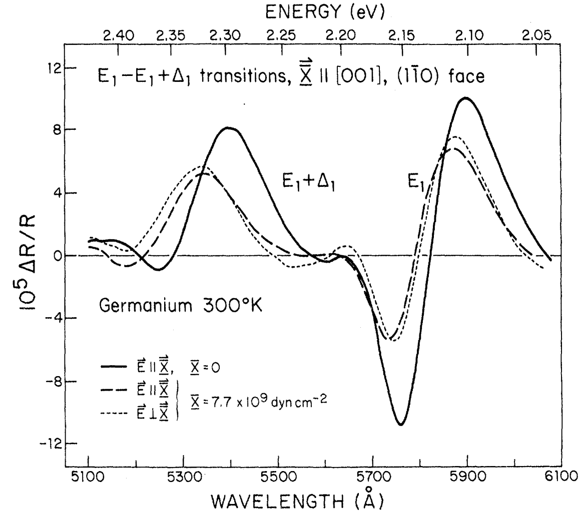

FIG. 14. Electroreflectance spectrum for the E_1 and $E_1+\Delta_1$ structure of Ge for zero stress and for a stress of 7.7×10^9 dyn cm^{-2} along [001] at 300 °K for light polarized parallel and perpendicular to the stress axis.

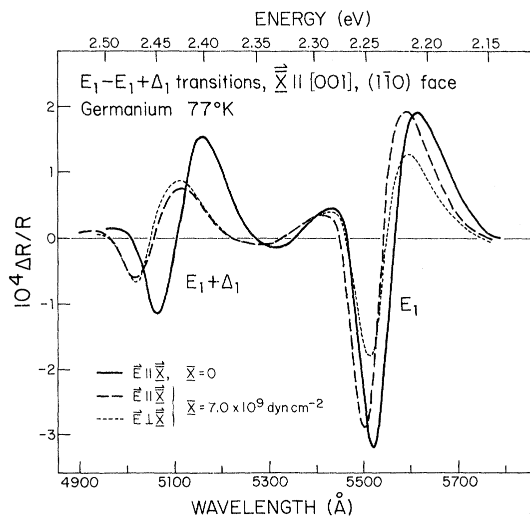

FIG. 13. Electroreflectance spectrum for the E_1 and $E_1+\Delta_1$ structure of Ge for zero stress and for a stress of 7.0×10^9 dyn cm^{-2} along [001] at 77 °K for light polarized parallel and perpendicular to the stress axis.

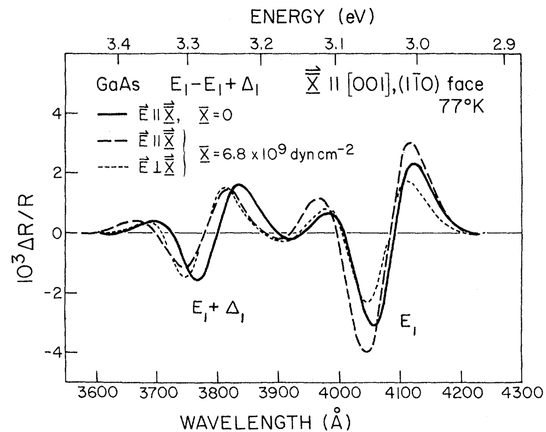

FIG. 15. E_1 and $E_1+\Delta_1$ electroreflectance peaks of GaAs at 77 °K for zero stress and a stress of 6.8×10^9 dyn cm^{-2} along [001] with light polarized parallel and perpendicular to the stress axis.

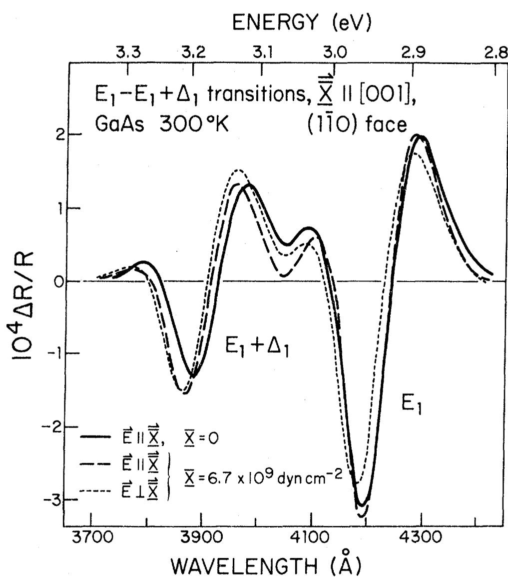

FIG. 16. E_1 and $E_1+\Delta_1$ electroreflectance peaks of GaAs at 300 °K for zero stress and a stress of 6.7×10^9 dyn cm^{-2} along [001] with light polarized parallel and perpendicular to the stress axis.

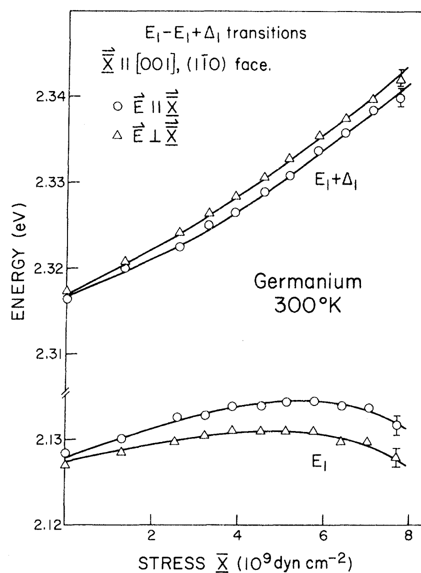

FIG. 18. Stress dependence of the energies of the E_1 and $E_1+\Delta_1$ peaks in Ge at 300 °K for $\vec{X}$ || [001] with light polarized parallel and perpendicular to the stress axis.

terms of the lower symmetry of the zinc-blende-type materials, e.g., linear $\vec{k}$ terms, since it is observed both in Ge and GaAs. However, the polarization-dependent splitting can be explained by including the electron-hole interaction, as has been done in Eq. (11).

In Figs. 17 and 18, we have plotted the energies of the $E_1 - E_1 + \Delta_1$ transitions for $\vec{X}$ || [001] for Ge at 77 and 300 °K, respectively, while in Figs. 19 and 20 we show the stress dependence of the $E_1 - E_1 + \Delta_1$ structure for $\vec{X}$ || [001] for GaAs at 77 and 300 °K, respectively. The energy values were obtained by

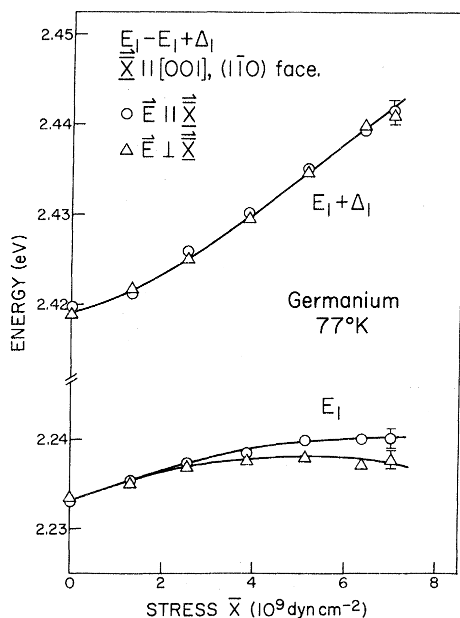

FIG. 17. Stress dependence of the energies of the E_1 and $E_1+\Delta_1$ peaks in Ge at 77 °K for $\vec{X}$ || [001] with light polarized parallel and perpendicular to the stress axis.

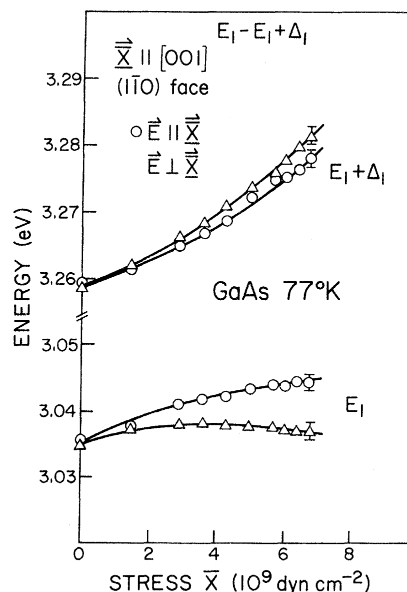

FIG. 19. Stress dependence of the energies of the E_1 and $E_1+\Delta_1$ peaks in GaAs at 77 °K for $\vec{X}$ || [001] with light polarized parallel and perpendicular to the stress axis.

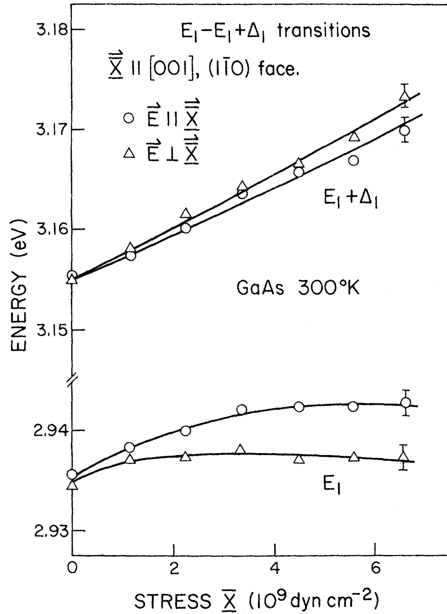

FIG. 20. Stress dependence of the energies of the E_1 and $E_1+\Delta_1$ peaks in GaAs at 300 °K for $\vec{X}$ || [001] with light polarized parallel and perpendicular to the stress axis.

the three-point method assuming a three-dimensional critical point.[7,46] These figures clearly show the linear stress dependence of the center of gravity, the nonlinear intraband effect, and the polarization-dependent splitting of the $E_1-E_1+\Delta_1$ structure at both temperatures. From these data we have obtained the values of D_1^1, D_3^3, δ_{J_1}, and δ_{J_2} for Ge and GaAs listed in Tables IV and V, respectively. The hydrostatic and intraband deformation potentials D_1^1 and D_3^3 respectively, were calculated using energy values at the center of gravity of the polarization split levels: D_1^1 was determined from the shift of the center of gravity of $E_1-E_1+\Delta_1$ while D_3^3 was obtained from the nonlinearity. The tabulated values of the deformation potentials were calculated using a least-squares fit. The parameters δ_{J1} and δ_{J2} were then calculated from the polarization-dependent splitting and the above value of D_3^3 [see Eqs. (16)]. For comparison we have also listed in Tables IV and V values of some of the above parameters as obtained from other experimental work, as well as values calculated from theoretical considerations.

An effective radii a_x for the exciton may be defined by[44]

$$P(0)=a_l^3/\pi a_x^3, \tag{17}$$

where a_l is the lattice constant. Assuming $J\approx\Delta_1$, we can estimate a_x from Eqs. (12) and (17) and the above values of δ_{J1} and δ_{J2}. The values of a_{x1} and a_{x2} thus obtained are also listed in Tables IV and V, for Ge and GaAs, respectively.

In both Ge and GaAs, there is little temperature dependence of the various parameters we have measured. We have also measured the splittings δ_{J1} and δ_{J2} at various values of the applied modulation voltage in order to correlate the magnitudes of the splittings with the electric field. Experimentally, it was found that they are independent of the applied field. In general, the values of the deformation potentials D_1^1 and D_3^3, as determined in this work, are in good agreement with previous work, with the exception of D_3^3 for Ge, for which we find a value considerably higher than that of prior workers.

We have also investigated the stress dependence of the linewidth and find that, to within experimental error, it is independent of stress.

Of particular importance is the observation that there exists a significant contribution of the electron-hole Coulomb interaction to the optical spectra of the $E_1-E_1+\Delta_1$ structure at room temperature. As discussed above this evidence is based solely on symmetry considerations and is not dependent on interpretations of the lineshape. The inclusion of the excitonic interaction should resolve the discrepancy in intensities and lineshapes between theoretical calculations and 300 °K-experimental-optical and modulated-optical properties of this structure in the diamond- and zinc-blende-type (DZB) semiconductors.[11] In addition, this interaction should be taken into account for resonance Raman effect associated with the $E_1-E_1+\Delta_1$ optical structure.[47]

A comparison of 300 °K measurements of the optical properties of DZB semiconductors in the $E_1-E_1+\Delta_1$ region with calculated curves obtained by a wide variety of techniques reveals a systematic discrepancy in intensity and line shape. As an illustration, Fig. 21 shows a theoretical curve of the imaginary part of the dielectric constant $\epsilon_2(\hbar\omega)$ for Ge. The calculation was based on the pseudopotential method which included energy and $l=2$ nonlocal effects as well as the usual local pseudopotential.[27] Also shown in Fig. 21 is 300 °K-experimental data. A similar discrepancy for this optical structure in the DZB substances is found for a number of different theoretical techniques.[19-27] Theory generates intensities which are significantly lower than experiment. In addition, close examination also shows a difference in lineshape. This is particularly evident in materials with a large spin-orbit splitting such as InSb and α-Sn. These differences have been attributed to exciton effects which are not taken into account in the calculations.[11] Although conclusive evidence for the excitonic nature of the $E_1-E_1+\Delta_1$ structure

at 77 °K in GaAs was presented several years ago,[18] it was crucial to verify the character of this optical feature at 300 °K since no systematic study of the low-temperature dc optical properties has been made, and hence, theory is generally compared to room-temperature data.

2. Stress parallel to [111]

A uniaxial stress along the [111] direction preferentially selects out the [111] direction (singlet), while making equal angles with the other three $[\bar{1}11], [\bar{1}1\bar{1}], [1\bar{1}\bar{1}]$ directions (triplet). This gives rise to an interband splitting between the singlet and the triplet. In addition, there is an intraband effect for the triplet states. The Hamiltonian matrix for the singlet [111] has no off-diagonal terms, (i.e., no intraband mixing) and can be written as[1]

$$\begin{array}{cc} \bar{U}_{v1} & \bar{U}_{v2} \end{array}$$
$$\begin{pmatrix} E_1 - \delta_H + \frac{1}{2}\delta_{S'} & 0 \\ 0 & E_1 + \Delta_1 - \delta_H + \frac{1}{2}\delta_{S'} \end{pmatrix}, \tag{18}$$

where δ_H is given by Eq. (13) and

$$\delta_{S'} = (1/\sqrt{3})D_1^5 S_{44} X. \tag{19}$$

The wave functions $\bar{U}_{v1}$ and $\bar{U}_{v2}$ are orbital wave functions taken so that $\bar{z}$ is along the [111] direction.

The energy eigenvalues for the singlet are

$$E_1^S(X) = E_1 - (D_1^1/\sqrt{3})(S_{11} + 2S_{12})X + \tfrac{1}{3}(\tfrac{1}{2}\sqrt{3})D_1^5 S_{44} X \tag{20a}$$

and

TABLE IV. Deformation potentials and spin-exchange parameters for the $E_1 - E_1 + \Delta_1$ transitions in germanium.

	Present work	Previous work	Theoretical calculations
D_1^1 (eV)	-9.6 ± 0.8 [a,b]	-9.7 ± 1.0 [c]	-6.9 [d]
	-8.2 ± 0.7 [e,b]	-9.9 ± 0.5 [f,g]	-8.6 [h]
	-8.1 ± 0.8 [e,f]	-7.8 ± 0.7 [i]	-8.1 [j]
D_1^5 (eV)	11.3 ± 1.1 [a,b]	7.5 ± 0.8 [c]	3.9 [d]
		5.9 ± 1.2 [f]	4.5 [d]
		8.5 ± 0.8 [i]	6.0 [h]
D_3^3 (eV)	5.8 ± 0.6 [e,b]	2.2 ± 0.7 [c]	
	5.9 ± 0.6 [e,k]	2.6 (at $\vec{k} = 0$) [i]	
D_3^5 (eV)	6.1 ± 1.5 [a,b]	1.5 ± 0.5 [c]	
		6.4 (at $\vec{k} = 0$) [i]	
δ_{J1} (eV)	$(3.4 \pm 0.4) \times 10^{-3}$ [e,b,l]		
	$(4.3 \pm 0.4) \times 10^{-3}$ [e,k,l]		
δ_{J2} (eV)	$(0 \pm 0.5) \times 10^{-3}$ [e,b,m]		
	$(2.0 \pm 0.2) \times 10^{-3}$ [e,k,m]		
a_{x1} (Å)	15.0 ± 1.0 [e,b]		
	13.9 ± 0.9 [e,k]		
a_{x2} (Å)	>20 [e,b,m]		
	18.0 ± 1.8 [e,k,m]		

[a] $\vec{X} \parallel [111]$.
[b] 77 °K.
[c] D. D. Sell and E. O. Kane, Phys. Rev. 185, 1103 (1969).
[d] P. J. Melz, Technical Report HP-25, Harvard University, Div. of Engineering and Applied Physics, Cambridge, Mass. (unpublished).
[e] $\vec{X} \parallel [001]$.
[f] U. Gerhardt, Phys. Rev. Lett. 15, 401 (1965); Phys. Status Solidi 11, 801 (1965).
[g] R. Zallen and W. Paul, Phys. Rev. 155, 703 (1967).
[h] L. R. Saravia and D. Brust, Phys. Rev. 178, 1240 (1969).
[i] Reference 28.
[j] F. Herman, R. Kortum, C. D. Kuglin, and R. A. Short, in *Quantum Theory of Solids: A Tribute to J. C. Slater*, edited by Per-Olov Lowdin (Academic, New York, 1966), p. 381.
[k] 300 °K.
[l] E_1 peak.
[m] $E_1 + \Delta_1$ peak.

$$E_1 + \Delta_1^S(X) = E_1 + \Delta_1 - (D_1^1/\sqrt{3})(S_{11} + 2S_{12})X + \tfrac{1}{3}(\tfrac{1}{2}\sqrt{3})D_1^5 S_{44} X. \quad (20b)$$

Using the wave functions with the proper transformations for the $[1\bar{1}\bar{1}]$, $[\bar{1}\bar{1}1]$, and $[\bar{1}1\bar{1}]$ bands, the Hamiltonian matrix for this triplet of equivalent bands under [111] stress may be written as

$$\begin{matrix} \bar{U}'_{v1} & \bar{U}'_{v2} \end{matrix}$$
$$\begin{pmatrix} E_1 - \delta_H - \frac{1}{6}\delta_{S'} & \frac{2}{3}\delta_{S''} \\ \frac{2}{3}\delta_{S''} & E_1 + \Delta_1 - \delta_H - \frac{1}{6}\delta_{S'} \end{pmatrix}, \quad (21)$$

where

$$\delta_{S''} = (1/\sqrt{6})D_3^5 S_{44} X. \quad (22)$$

Solving for the eigenvalues, and expanding in powers of $\delta_{S''}/\Delta_1$ we find

$$E_1^T(X) = E_1 - (D_1^1/\sqrt{3})(S_{11} + 2S_{12})X - (1/6\sqrt{3})D_1^5 S_{44} X - \tfrac{2}{27}[(D_3^5)^2/\Delta_1]S_{44}^2 X^2 + \cdots \quad (23a)$$

and

$$E_1 + \Delta_1^T(X) = E_1 + \Delta_1 - (D_1^1/\sqrt{3})(S_{11} + 2S_{12})X - (1/6\sqrt{3})D_1^5 S_{44} X + \tfrac{2}{27}[(D_3^5)^2/\Delta_1]S_{44}^2 X^2 + \cdots. \quad (23b)$$

The E_1 and $E_1 + \Delta_1$ transitions under a [111] uniaxial stress show a hydrostatic shift in the energy (δ_H term) and an interband splitting that splits the four equivalent bands into a singlet and a triplet state ($\delta_{S'}$ term). The singlet state is linear in stress [see Eq. (20)], and is seen only for light polarized perpendicular to the direction of stress ($\vec{E} \perp \vec{X}$).[28] The triplet state has a linear-hydrostatic and shear component, and a nonlinearity due to intraband mixing [see Eq. (23)]. It is seen for light polarized both parallel and perpendicular to the stress direction. The intraband mixing terms are equal and opposite between the E_1 and $E_1 + \Delta_1$ bands for the triplet.

It is possible to introduce an exchange interaction term for the triplet state. However, the nonlinearity observed is very small in energy for Ge and unobservable for GaAs. The exchange splitting

TABLE V. Deformation potentials and spin-exchange parameters for the $E_1 - E_1 + \Delta_1$ transitions in gallium arsenide.

	Present work	Previous work	Theoretical calculations
D_1^1 (eV)	-7.6 ± 0.5 [a,b]	-6.9 ± 0.7 [c,d]	-14.4 [e]
	-7.9 ± 0.5 [f,b]	-9.4 ± 0.9 [g,h]	
	-6.7 ± 0.6 [f,h]	-8.0 ± 0.8 [h,i]	
		-9.3 [j]	
D_1^5 (eV)	9.2 ± 0.9 [a,b]	6.2 ± 0.6 [c,d]	7.9 ± 0.5 [e]
		8.5 ± 0.8 [g,h]	
D_3^3 (eV)	3.4 ± 0.3 [f,b]	3.2 ± 0.3 [b,i]	
	3.5 ± 0.3 [f,h]	2.4 (at $\vec{k} = 0$) [g]	
D_3^5 (eV)	0 ± 0.5 [a,b]	8.5 (at $\vec{k} = 0$) [g]	
δ_{J1} (eV)	$(10.2 \pm 1.0) \times 10^{-3}$ [f,b,k]	10×10^{-3} [i,b,k]	
	$(9.9 \pm 1.0) \times 10^{-3}$ [f,h,k]		
δ_{J2} (eV)	$(5.5 \pm 0.8) \times 10^{-3}$ [f,b,l]	10×10^{-3} [i,b,l]	
	$(3.6 \pm 0.5) \times 10^{-3}$ [f,h,l]		
a_{x1} (Å)	10.7 ± 0.6 [f,b,k]		
	10.6 ± 0.6 [f,h,k]		
a_{x2} (Å)	12.2 ± 1.0 [f,b,l]		
	15.2 ± 1.0 [f,b,l]		

[a] $\vec{X}$ ∥ [111].
[b] 77 °K.
[c] D. D. Sell and S. E. Stokowski, in *Proceedings of the Tenth International Conference on the Physics of Semiconductors, Cambridge*, 1970 (U. S. AEC, 1970), p. 417.
[d] 2 °K.
[e] P. J. Melz, Technical Report HP-25, Harvard University, Div. of Engineering and Applied Physics, Cambridge, Mass. (unpublished).
[f] $\vec{X}$ ∥ [001].
[g] Reference 28.
[h] 300 °K.
[i] Reference 18.
[j] M. I. Wolfe, Thesis (Yeshiva University, 1973) (unpublished).
[k] E_1 peak.
[l] $E_1 + \Delta_1$ peak.

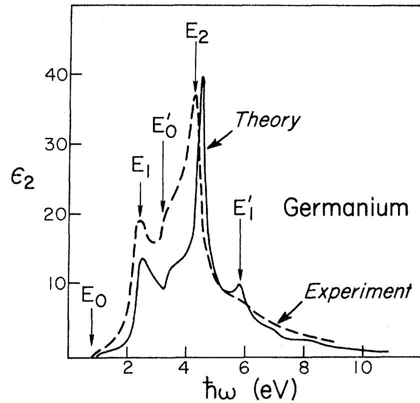

FIG. 21. Calculated imaginary part of the dielectric function $\epsilon_2(\hbar\omega)$ (dashed lines) from Ref. 27, and experimental $\epsilon_2(\hbar\omega)$ (solid lines) from H. R. Phillip and H. Ehrenreich, Phys. Rev. 129, 1550 (1963) for Ge. Spin-orbit effects have not been included. Note the difference in intensity for the E_1 peak.

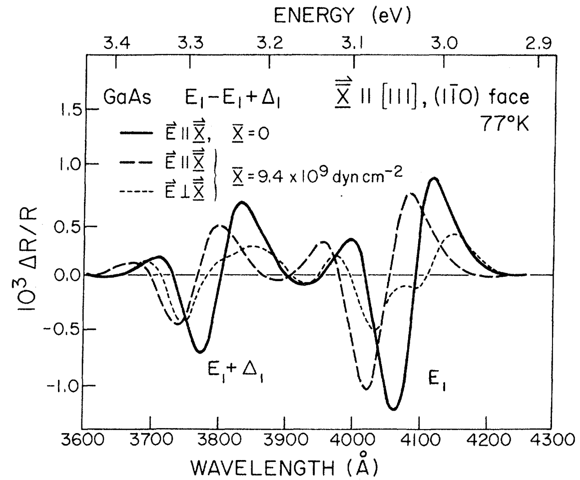

FIG. 23. Electroreflectance spectrum of the E_1 and $E_1+\Delta_1$ structure of GaAs for zero stress and a stress of 9.4×10^9 dyn cm^{-2} along [111] at 77 °K for light polarized parallel and perpendicular to the stress axis.

is seen because both the nonlinearity and exchange exist together [see, for example, Eq. (16)]. Since the nonlinearity is very small, no splitting is expected within experimental error and was not observed experimentally. Therefore the exchange interaction was not introduced in the above formulation.

Figures 22 and 23 show the electroreflectance spectra of the $E_1 - E_1 + \Delta_1$ peaks of Ge and GaAs, respectively, at 77 °K with $\vec{X} \parallel [111]$ and light polarized parallel and perpendicular to the stress axis. For the latter polarization, the splitting of the E_1 peak is clearly evident in both materials. For the $E_1 + \Delta_1$ structure a splitting is clearly resolved for Ge while for GaAs, which has a greater lifetime broadening, the separation of the stress-induced structure is not clearly resolved.

Plotted in Figs. 24 and 25 are the energies of the $E_1 + \Delta_1$ structure as a function of [111] stress for Ge and GaAs, respectively, with light polarized parallel and perpendicular to the stress axis. In the case of Ge for $X < 7\times10^9$ dyn cm^{-2} the energies of the E_1 and $E_1+\Delta_1$ triplet state do not agree for the two polarizations, the $\perp$ polarization being lower than the $\parallel$ case. This is due to the fact that the stress has not yet completely resolved the singlet and

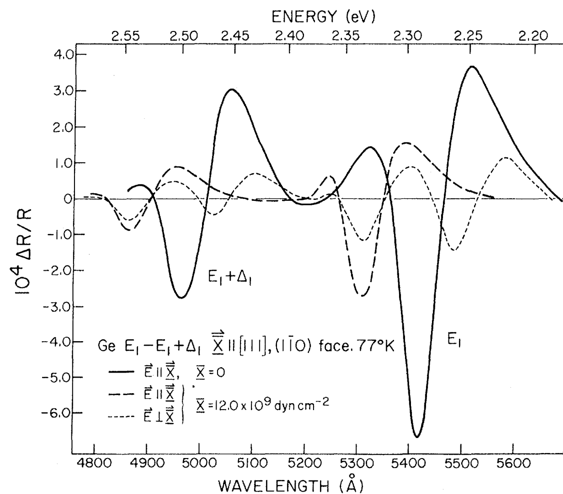

FIG. 22. Electroreflectance spectrum of the E_1 and $E_1+\Delta_1$ structure of Ge for zero stress and a stress of 12.0×10^9 dyn cm^{-2} along [111] at 77 °K for light polarized parallel and perpendicular to the stress axis.

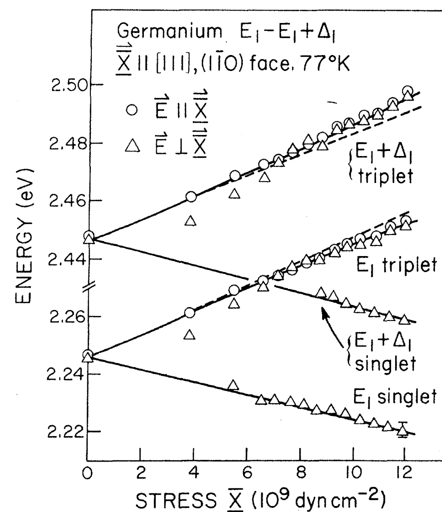

FIG. 24. Stress dependence of the energies of the E_1 and $E_1+\Delta_1$ electroreflectance peaks in Ge at 77 °K for $\vec{X} \parallel [111]$ with light polarized parallel and perpendicular to the stress axis.

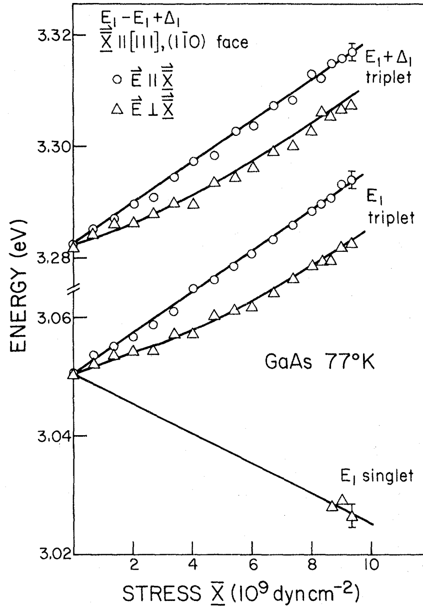

FIG. 25. Stress dependence of the energies of the E_1 and $E_1+\Delta_1$ electroreflectance peaks in GaAs at 77 °K for $\vec{X}\,||\,[111]$ with light polarized parallel and perpendicular to the stress axis.

triplet. For $X > 7\times 10^9$ dyn cm^{-2} the energies agree for the two polarizations. The dashed lines in Fig. 24 are the linearized stress dependence of the E_1 and $E_1+\Delta_1$ triplet. In agreement with Eq. (23), the nonlinearity due to the intraband mixing is clearly evident in the repulsion between E_1 and $E_1+\Delta_1$ for the triplet. The E_1 and $E_1+\Delta_1$ singlet have a linear stress dependence [see Eq. (20)]. For GaAs, the situation is somewhat more complicated due to the greater lifetime broadening of this material. Even at the highest stresses the singlet and triplet are not completely resolved for $\vec{E}\perp\vec{X}$ (see Fig. 23) and hence the energies of the triplet for the two polarizations do not agree (see Fig. 23 and 25). Note also that there is no nonlinearity of either triplet state for GaAs and hence no exchange splitting was observed. For both Ge and GaAs, the data of Figs. 24 and 25 were obtained from the higher energy peak positions of each of the E_1 and $E_1+\Delta_1$ transitions. In principle, either the lower- or higher-energy peaks could be used but since the higher-energy one is sharper relative to the lower-energy one it is more accurate. The three point method was not used since the line shapes are modified by the splittings for $\vec{E}\perp\vec{X}$.

From the stress dependence of the E_1 and $E_1+\Delta_1$ transitions shown in Figs. 24 and 25 we have determined the parameters D_1^1, D_1^5, and D_3^5 which are listed in Tables IV and V for Ge and GaAs, respectively. The values were obtained using a least-squares fit to the data. For GaAs, D_1^1 and D_1^5 were calculated from the splittings between the singlet and the $\vec{E}\,||\,\vec{X}$ triplet since it was found that this procedure gives a value of D_1^1 that agrees closely with that obtained for [001] stress. The position of the singlet is therefore indicative of complete resolution. We have found that within experimental error there is no difference for D_1^1 and D_1^5 associated with both the E_1 and $E_1+\Delta_1$ transitions. For both materials D_1^1 was in good agreement with the value found for [001] stress and other experiments. D_1^5 in Ge is substantially larger than previous values. In comparison with the experiments by Pollak and Cardona,[28] the resolution of the present experiment is much higher, permitting a clear splitting in the peaks that was not obtained in their experiment. Since the singlet is three times as weak as the triplet, it will appear higher in energy than its real energy, being "pulled" towards the triplet, if it is not completely resolved. The splitting in energy would therefore be artificially smaller, giving a smaller value for D_1^5. It is believed that the increased resolution and the consequent well-defined splitting is the reason for obtaining a higher value of D_1^5 than that previously obtained. From [111] stress data, therefore, it is possible to obtain the deformations potentials D_1^1 (hydrostatic), D_1^5 (interband), and D_3^5 (intraband). The existence of the interband splitting, which is due to the removal of the equivalence of the four ⟨111⟩ bands, confirms that the transitions are along the $\Lambda(\langle 111\rangle)$ directions.

IV. CONCLUSIONS

From the effects of uniaxial stress on SBER of the $E_0 - E_0+\Delta_0$ optical structure we have been able to measure the orbital and spin-dependent shear-deformation potentials as well as the hydrostatic-deformation potential of the lowest direct gap in Ge and GaAs. The orbital and hydrostatic-deformation potentials are in good agreement with previously reported values. For GaAs, the spin-dependent shear-deformation potentials have been measured for the first time, while for Ge, our value for this parameter is found to be in good agreement with cyclotron resonance work. Interband reduced masses for the direct edge in Ge were measured at high stresses from the Franz-Keldysh oscillations of the E_0 electroreflectance structure.

The experiments on the $E_1 - E_1+\Delta_1$ structure have revealed the existence of an electron-hole Coulomb interaction at 300 °K. This observation should contribute to resolving the discrepancy in intensity and lineshape between theoretical calculations and experimental results for the optical properties of this transition. The results of our experiment also gives weight to the interpretation of the lineshape

of the modulated optical spectra of the $E_1 - E_1 + \Delta_1$ structure in terms of the electron-hole interaction rather than a combination of M_0- and M_1-critical points which do not include excitonic effects. In addition, we have measured the hydrostatic and shear (inter- and intraband) deformation potentials and spin-exchange parameters of this optical structure.

---

†Supported by the National Science Foundation.

*Formerly M. Chandrapal.

‡Present address: Max-Planck Institut fur Festkorperforschung; 7 Stuttgart 80; Fed. Rep. Germany.

[1]See, for example, F. H. Pollak, Surf. Sci. 37, 863 (1973); and refereces therein.

[2]I. Balslev, *Semiconductors and Semimetals,* edited by R. K. Willardson and A. C. Beer (Academic, New York, 1972), Vol. 9, p. 403.

[3]M. Cardona, *Modulation Spectroscopy,* edited by F. Seitz, D. Turnbull, and H. Ehrenreich (Academic, New York, 1969); and references therein.

[4]Y. Hamakawa and T. Nishino, in *Optical Properties of Solids—New Developments,* edited by B. O. Seraphin (North-Holland, Amsterdam, 1976).

[5]B. O. Seraphin, in *Semiconductors and Semimetals,* edited by R. K. Willardson and A. C. Beer (Academic, New York, 1972), Vol. 9, p. 1; and references therein.

[6]J. E. Fischer and D. E. Aspnes, Phys. Status Solidi 55, 9 (1973); and references therein.

[7]D. E. Aspnes, Phys. Rev. Lett. 28, 913 (1972).

[8]D. E. Aspnes and A. A. Studna, Phys. Rev. B 7, 4605 (1973).

[9]D. E. Aspnes, Surf. Sci. 37, 418 (1973); and references therein.

[10]See, for example, J. C. Phillips, *Bonds and Bands in Semiconductors* (Academic, New York, 1973); and references therein.

[11]M. Chandrapal and F. H. Pollak, Solid State Commun. 18, 1263 (1976); and references therein.

[12]J. C. Phillips, Solid State Phys. 18, 56 (1966).

[13]M. Cardona and G. Harbeke, J. Appl. Phys. 34, 813 (1963).

[14]B. Velicky and J. Sak, Phys. Status Solidi 16, 147 (1966).

[15]C. Duke and B. Segall, Phys. Rev. Lett. 17, 19 (1966).

[16]Y. Toyozawa, M. Inoue, T. Inoui, M. Okazaki, and E. Hanamura, Proc. Phys. Soc. Jpn. 21, 133 (1967).

[17]E. O. Kane, Phys. Rev. 180, 852 (1969).

[18]J. E. Rowe, F. H. Pollak, and M. Cardona, Phys. Rev. Lett. 22, 933 (1969).

[19]M. L. Cohen and V. Heine, Solid State Phys. 24, 37 (1970); and references therein.

[20]F. Herman, R. L. Kortum, C. F. Kuglin, J. P. Van Dyke, and S. Skillman, in *Methods in Computational Physics,* edited by B. Adler, S. Fernbach, and M. Rotenberg (Academic, New York, 1968), Vol. 8, p. 193; and references therein.

[21]F. H. Pollak, M. Cardona, C. W. Higginbotham, F. Herman, and J. P. Van Dyke, Phys. Rev. B 2, 352 (1970).

[22]G. Dresselhaus and M. Dresselhaus, Phys. Rev. 160, 649 (1967).

[23]F. H. Pollak, C. W. Higginbotham, and M. Cardona, *Proceedings of the International Conference on the Physics of Semiconductors, Moscow, 1968* (Nanba, Leningrad, 1968), p. 57; and references therein.

[24]D. J. Stukel and R. N. Euwema, Phys. Rev. B 1, 1635 (1970).

[25]T. C. Collins, D. J. Stukel, and R. N. Euwema, Phys. Rev. B 1, 724 (1970).

[26]J. P. Van Dyke, Phys. Rev. B 5, 1489 (1972).

[27]W. D. Grobman, D. E. Eastman, and J. L. Freeouf, Phys. Rev. B 12, 4405 (1975).

[28]F. H. Pollak and M. Cardona, Phys. Rev. 172, 816 (1968).

[29]K. Suzuki and J. C. Hensel, Phys. Rev. B 9, 4184 (1974); and references therein.

[30]J. C. Hensel and K. Suzuki, Phys. Rev. B 9, 4219 (1974); and references therein.

[31]P. Handler, S. Jasperson, and S. Koeppen, Phys. Rev. Lett. 23, 1387 (1969).

[32]M. Chandrapal, Ph.D. thesis (Brown University, 1976) (unpublished).

[33]C. R. Pidgeon and S. H. Groves, Phys. Rev. 186, 824 (1969).

[34]W. Wardzynski and M. Suffczynski, Solid State Commun. 10, 417 (1972).

[35]In GaAs we have neglected C_2, the stress-induced coupling between the Γ_1 conduction bands and the $M_J = \pm\frac{1}{2}$ valence bands for $\vec{X} \| [111]$ or $\vec{X} \| [110]$. See, for example, D. G. Seiler and K. L. Hathcox, Phys. Rev. Lett. 29, 647 (1972).

[36]F. Evangelisti, A. Frova, and J. U. Fischbach, Phys. Rev. Lett. 29, 1001 (1972).

[37]P. J. Melz and I. B. Ortenburger, Phys. Rev. B 3, 3257 (1971).

[38]R. Bendorius and A. Shileika, Solid State Commun. 8, 1111 (1970).

[39]L. D. Laude, F. H. Pollak, and M. Cardona, Phys. Rev. B 3, 2624 (1971).

[40]D. Brust and L. Liu, Solid State Commun. 4, 193 (1966).

[41]F. Cerdeira, J. S. DeWitt, U. Rossler, and M. Cardona, Phys. Status Solidi 41, 735 (1970).

[42]G. G. Wepfer, T. C. Collins, and R. N. Euwema, Phys. Rev. B 4, 1296 (1971).

[43]D. E. Aspnes, Phys. Rev. B 10, 4228 (1974), and refernces therein.

[44]E. O. Kane, Phys. Rev. 178, 1368 (1969).

[45]R. J. Elliott, Phys. Rev. Lett. 27, 188 (1971).

[46]D. E. Aspnes, Phys. Rev. Lett. 27, 188 (1971).

[47]See, for example, M. Cardona, Surf. Sci. 37, 100 (1973); and K. P. Jain and G. Choudhury, Phys. Rev. B 8, 676 (1973).